



# Iron metal-organic framework nanofiber membrane for the integration of electro-Fenton and effective continuous treatment of pharmaceuticals in water

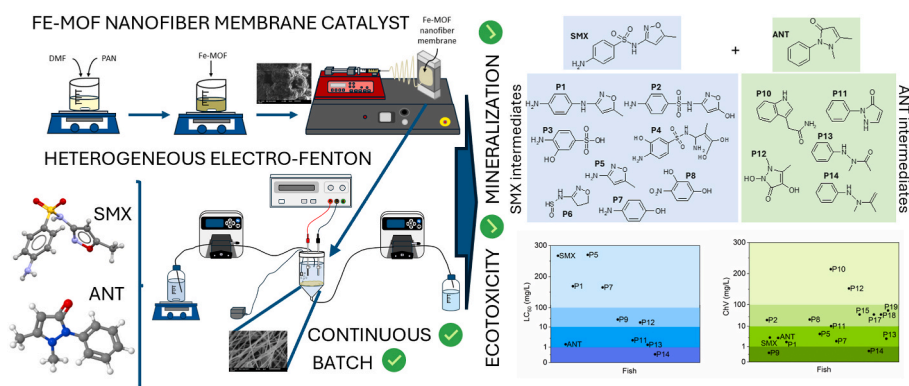
Barbara Lomba-Fernández, Antía Fdez-Sanromán, Marta Pazos, M. Angeles Sanromán, Emilio Rosales\*

CINTECX, Universidade de Vigo, Grupo de Bioingeniería y Procesos Sostenibles, Departamento de Ingeniería Química, Campus Lagoas-Marcosende, 36310, Vigo, Spain

## HIGHLIGHTS

- Successful Fe-MOF nanofiber membranes created with cutting-edge electrospinning.
- Fe-MOF nanofiber proves high catalytic activity for electro-Fenton drug degradation.
- Remarkable stability and durability of the membrane under batch and continuous system.
- In-silico analysis of intermediates confirms the toxicity reduction in treated water.

## GRAPHICAL ABSTRACT



## ARTICLE INFO

Handling Editor: Am Jang

**Keywords:**  
Fe-MOF nanofiber membrane  
Electro-Fenton  
Flow system degradation  
Antipyrine  
Sulfamethoxazole

## ABSTRACT

In this study, an iron metal-organic framework (Fe-MOF) was synthesized and immobilized by electrospinning technique with the objective of obtaining a membrane composed of nanofibers of this material (Fe-MOF nanofiber membrane). The characterization performed by XRD, TEM, SEM, EDS mapping and FTIR confirmed the correct synthesis of Fe-MOF as well as its correct retention in the elaborated membranes. The usefulness and effectiveness of the Fe-MOF nanofiber membrane as a catalyst for the electro-Fenton process was evaluated by performing sulfamethoxazole degradation tests. Different parameters such as the effect of intensity (25 and 100 mA), the effect of the drug initial concentration (10–50 mg/L) and the reusability of membranes were studied. Then, the degradation of a drug mixture formed by sulfamethoxazole and antipyrine was evaluated, reaching a degradation of 92.10 % and 87.43 % respectively for each drug in 4 h at 25 mA. In addition, the identification of reactive oxygen species was ascertained by scavenger assays. The study of degradation products was also carried out and their toxicity was predicted by ECOSAR program, concluding that the environmental toxicity would disappear with mineralization. Finally, given the good results obtained in batch tests, the behavior of the process

\* Corresponding author.

E-mail addresses: [barbara.lomba.fernandez@uvigo.gal](mailto:barbara.lomba.fernandez@uvigo.gal) (B. Lomba-Fernández), [antia.fernandez.sanroman@uvigo.gal](mailto:antia.fernandez.sanroman@uvigo.gal) (A. Fdez-Sanromán), [mcurras@uvigo.es](mailto:mcurras@uvigo.es) (M. Pazos), [sanroman@uvigo.es](mailto:sanroman@uvigo.es) (M.A. Sanromán), [emilirov@uvigo.es](mailto:emilirov@uvigo.es) (E. Rosales).

<https://doi.org/10.1016/j.chemosphere.2024.143447>

Received 1 August 2024; Received in revised form 20 September 2024; Accepted 30 September 2024

Available online 2 October 2024

0045-6535/© 2024 The Authors. Published by Elsevier Ltd. This is an open access article under the CC BY-NC license (<http://creativecommons.org/licenses/by-nc/4.0/>).

was studied in a system that works continuously, achieving a stable degradation of 83.10 % in the case of treatment with a mixture of drugs. This confirmed the stability of the Fe-MOF nanofiber membrane, as well as, its catalytic activity, making it suitable for long-term treatments.

## 1. Introduction

According to the World Health Organization, \$1170 billion was spent on global pharmaceuticals in 2021 alone, highlighting their widespread. Effluents from the pharmaceutical industry, hospitals and homes are primary sources of environmental contamination, with inadequate disposal contributing less (dos Santos et al., 2021; Huang et al., 2019; Szekeres et al., 2018). Water pollution from pharmaceuticals poses a serious environmental concern, driving the need for innovative remediation technologies (Gopinath et al., 2022a). Advanced oxidation processes (AOPs) stand out as a promising solution in the field of efficacy in eliminating a wide range of environmental pollutants (Tang et al., 2024). Heterogeneous electro-Fenton processes have received significant attention in several studies for their high efficiency (Liu et al., 2023b, 2023c; Song et al., 2022). These processes harness the power of electrochemistry to generate highly reactive hydroxyl radicals on the surface of solid catalysts, which effectively degrade recalcitrant organic pollutants in water (Brillas, 2022; Heidari et al., 2023). Its heterogeneous nature facilitates the catalyst recycling and broader operational parameters, such as pH, widening its applicability (Brillas, 2022; Gopinath et al., 2022).

One of the key parameters in these processes is the proper selection of the catalyst. Metal-Organic Frameworks (MOFs) stands out due to their exceptional properties (Badea and Niculescu, 2022; Rojas and Horcajada, 2020). MOFs are a class of porous crystalline materials constructed from groups of metal ions coordinated with organic linkers (Fdez-Sanromán et al., 2022; Jin et al., 2020). They exhibit clear advantages, including a highly adjustable porosity, vast surface areas and many functional groups (Liu et al., 2023a; Oladoye et al., 2021). Due to their excellent properties, they are widely used in a variety of applications, such as energy and gas storage, environmental treatment or biomedicine (Boorboor Ajdari et al., 2020; Petit, 2018; Sharabati et al., 2022). Initially, these MOFs were synthesized with a single metal in the center of the structure. Nowadays, some studies reinforce the catalytic properties of these materials by adding one or more metals to the structure (Fdez-Sanromán et al., 2023b). Among them, iron-derived MOFs, characterized by highly adjustable porosity, a large surface and open metal sites, have attracted the attention of the scientific community as catalysts and adsorbents (Du and Zhou, 2021; Sirés and Brillas, 2021). These materials provided excellent performance in modified cathodes and suspension catalysts for environmental remediation (Du et al., 2022, 2023), but more studies are needed to improve these materials and advance their applicability in electro-Fenton processes. Despite its remarkable properties, their powder form hinders continuous flow system operations, necessitating effective immobilization techniques. Electrospinning emerges as a versatile fabrication method for the immobilization of MOFs, producing nanofibers with high surface area-to-volume ratios (Subash et al., 2022; Uddin et al., 2022). By this method, nanofibers are produced, forming an interconnected pore matrix by applying an electric field to a jet of a polymer solution (Khalf and Madhally, 2017; Li et al., 2021). A great diversity of polymers (natural, synthetic, or a mixture of both) can be used for their formation (Agarwal et al., 2008). The process is influenced by various parameters among which stand out the properties of polymer solution (conductivity, viscosity, surface tension and molecular weight), applied electric field, flow rate, tip-distance collector, temperature and humidity of the environment. Thus, depending on these parameters the type of fiber that can be obtained can be totally different (Bhardwaj and Kundu, 2010; Subash et al., 2022). By leveraging electrospinning, researchers have successfully developed fibers with exceptional features such as large surface

area, high porosity and the ability to be functionalized with various substances, making this technology a cornerstone in the development of advanced materials (Zhang et al., 2023). In particular, the immobilization of metals on electrospinning nanofibers has revolutionized applications such as environmental remediation, catalysis, and sensing (Gong et al., 2020; Yu et al., 2021).

This work delves into the synthesis of a mixed matrix membrane of Fe-MOF nanofiber. The incorporation of Fe-MOF into the membrane not only addresses the problems related to the practical use of MOF powders, such as poor separation and recyclability, but also synergistically could improve the overall degradation performance of the system operating in a continuous flow system. In this study, the correct immobilization of Fe-MOF in the polymeric matrix was assessed by analyzing the characteristics of the resulting membrane and evaluating its efficiency in removing two pharmaceuticals, sulfamethoxazole (SMX) and antipyrine (ANT). All of this with the final aim of operating in a continuous flow system, thus offering a cutting-edge solution to a pressing environmental problem.

## 2. Materials and methods

### 2.1. Materials and reagents

The reagents used for the synthesis of the catalytic system were N, N-dimethylformamide (DMF, 99%), 2-aminoterephthalic acid (NH<sub>2</sub>BDC), iron (II) sulphate heptahydrate (FeSO<sub>4</sub>•7H<sub>2</sub>O), polyacrylonitrile (PAN) and ethanol. SMX and ANT were used as model contaminants and sodium sulphate anhydrous (Na<sub>2</sub>SO<sub>4</sub>) as electrolyte. For the determination of specific reactive oxygen species (ROS), tert-butanol (TBA, ≥99%), furfural (FFA, 99%) and *p*-benzoquinone (PBQ, ≥98%) were used. All these reagents were supplied by Sigma Aldrich (Madrid, Spain).

### 2.2. Synthesis of Fe-MOF nanofiber membrane

To carry out the Fe-MOF synthesis, the procedure indicated in the study by Fu et al. (2022) was followed with slight modifications. Its immobilization was conducted using the electrospinning technique (Fdez-Sanromán et al., 2023a). Initially, 0.8 g of PAN were homogeneously dissolved with 10 mL of DMF for 4 h at 70 °C. Subsequently, 0.1 g of Fe-MOF were mixed for 12 h until complete homogenization (Figure SM1).

### 2.3. Characterization of the Fe-MOF nanofiber membrane

The surface characterization of the catalyst and synthesized nanofibers was performed by scanning electron microscopy and energy dispersive spectrometry (SEM/EDS) using a JEOL JSM6010LA with EDS Oxford AZtecOne SEM and a JEOL JEM-1010 (100 kV). Fourier transform infrared spectroscopy (FTIR) was performed on a Nicolet 6700 spectrometer. Finally, X-ray diffraction (XRD) was conducted using a Siemens D5000 diffractometer (Ks Analytical Systems, United States).

The wettability of the nanofibers surface was determined by measuring the water contact angle with a Kruss MobileDrop HG11 equipment together with the DSA2 software.

### 2.4. Degradation experimental methods

#### 2.4.1. Batch system setup

Anodic oxidation and electro-Fenton tests were performed with each drug (SMX and ANT) and with a mixture of both. All experiments were

performed in a 100 mL cylindrical cell with an operating volume of 75 mL. The anode selected was a boron doped diamond electrode (BDD, Boromond) and the cathode a titanium electrode (Polymet) with modified surface by sandblasting. The size of both electrodes was  $3 \times 4$  cm and the separation between them was 2 cm. The electric field was applied through a power supply (E3612A 30W, Agilent). All solutions used in the experiments had a concentration of 10 mM of  $\text{Na}_2\text{SO}_4$  to improve their conductivity. Fe-MOF nanofiber was only added in electro-Fenton tests. The amount of Fe-MOF nanofiber used in each test was 0.10 g and was placed between both electrodes. Moreover, in the electro-Fenton the aeration was supplied by a tank pump (APS300, Tetra), maintaining a constant flow rate of 0.5 L/min. Samples were collected during the experiment to determine the progress of drug elimination. All the results are the average of duplicated assays, and the standard deviations were below 5%.

#### 2.4.2. Continuous system setup

Figure SM2 shows a diagram with the numbered elements of the corresponding assembly for the continuous test. The electrochemical cell was similar that described in batch procedure. The flow rate was established to operate at two residence time of the polluted water, 3.35 and 8.5 h.

#### 2.4.3. Scavengers assays

The effects of ROS on drug degradation were determined to better understand its mechanism. To do that, performing masking experiments, in the same working conditions as described in section 2.4.1. and 25 mA. TBA (50 mM), FFA (50 mM) and PBQ (10 mM) were used because they react with hydroxyl ( $\text{HO}\cdot$ ), singlet ( $^1\text{O}_2$ ) and hydroxyl, and superoxide ( $\text{O}_2^-$ ), respectively.

### 2.5. Analytical procedures

#### 2.5.1. HPLC determination

The concentration of drugs, carboxylic acids and phenols were determined with HPLC Agilent 1260 equipped with a ZORBAX Eclipse XDB-C8, Rezex<sup>TM</sup> ROA-Organic Acid H+ and Synergi<sup>TM</sup> Polar-RP 80 Å columns, respectively. The detector used was a Diode Array Detector operating at 263 nm for SMX, 242 nm for ANT and 210 nm for carboxylic acids. Phenols were detected at 266, 290, 274, 276 and 256 nm.

#### 2.5.2. Identification of degradation intermediates

The degradation intermediates of the electro-Fenton process were identified by Liquid Chromatography-Mass Spectrometry using a Hewlett-Packard 5989 equipped with a ZORBAX Eclipse XDB-C18.

#### 2.5.3. Iron determination

The determination of the iron content after experiments was carried out by Inductively Coupled Plasma-Optical Emission Spectrometry (ICP-OES), using a Thermo Scientific<sup>TM</sup> iCAP<sup>TM</sup> PRO XP DUO.

### 2.6. Toxicity evaluation

Acute ( $\text{LC}_{50}$ ) and chronic (ChV) toxicity endpoints for fish, aquatic invertebrates (*Daphnia*), and aquatic plants (*Green algae*) of the SMX, ANT and their intermediates were ascertained using an Estimation Software Tool, ECOSAR 2.2 (EPA).

## 3. Results and discussion

#### 3.1. Fe-MOF nanofiber membrane preparation and characterization

Initially, the synthesized Fe-MOF was characterized to analyze its structure and check the correct formation of the catalyst (Figure SM3). Once the correct synthesis of the Fe-MOF was confirmed (Figure SM3), the Fe-MOF nanofiber membrane was prepared, varying three

conditions: flow rate, voltage and distance between needle and collector. Thus, flow rates from 1 to 2.5 mL/h were tested, the voltage was varied in a range of 15–20 kV and three distances between the needle and the collector were tried: 12, 15 and 21 cm. Finally, after several failed tests (Table SM1), it was determined that the optimal conditions for the elaboration of the Fe-MOF nanofiber membranes were: flow rate of 2 mL/h, voltage of 18 kV and needle-collector distance of 15 cm.

The Fe-MOF nanofiber membrane was then characterized to verify a proper immobilization. For this purpose, the functional groups of Fe-MOF, PAN membrane and Fe-MOF nanofiber membrane were explored through FTIR spectra (Fig. 1a). The spectra of the compounds revealed vibration bands characteristic of Fe-MOF and PAN, confirming that the composite fibers were a blend of the source materials. In the Fe-MOF membrane, the sharp and strong intensity of the absorption peak at  $2243\text{ cm}^{-1}$  was attributed to the presence of the nitrile functional group ( $\text{C}\equiv\text{N}$ ) (Hussain et al., 2021; Pujiarti et al., 2023; Zhang et al., 2020). Peaks appearing in the range  $2851\text{ cm}^{-1}$ – $2922\text{ cm}^{-1}$  indicate C–H bond stresses in  $\text{CH}_2$  and  $\text{CH}_3$  groups, while those present between  $1070\text{ cm}^{-1}$ – $900\text{ cm}^{-1}$  would correspond to bond stresses C–C and C–CN (Fdez-Sanromán et al., 2024; Hussain et al., 2021). Peaks at 1623, 1492 and  $1255\text{ cm}^{-1}$  are related to the presence of Fe-MOF corresponding to the frame stretching vibration, the  $\text{C}=\text{C}$  vibration, and amine groups C–N vibration of the benzene ring. The band at  $750\text{ cm}^{-1}$  was assigned to the vibrations of the C–H and the band at  $513\text{ cm}^{-1}$  correspond to the Fe–O stretching mode due to the bonding of iron centers and organic ligands. Thus, the presence of characteristic peaks associated with Fe-MOF and with the PAN polymer material used for immobilization in the Fe-MOF nanofiber membrane spectrum confirmed the generation and stability of Fe-MOF in the membrane made using the electro-spinning technique.

SEM was used to determine the morphology of the prepared membranes. Fig. 1b and c presents the SEM images of the PAN membrane and the Fe-MOF nanofiber membrane, respectively. The images revealed that the PAN membrane is composed of long fibers that were continuous and cylindrically shaped (Fig. 1b). By adding the Fe-MOF to the polymer matrix the fibers showed a larger diameter and more roughness compared to the PAN fibers (Fig. 1c). In addition, small agglomerations can be seen in this same figure which confirmed that the Fe-MOF particles were incorporated into the membrane providing more active sites for the removal of contaminants. The morphology and shape of the fibers observed are consistent with other studies already conducted by different authors (Ramezani et al., 2020; Zhang et al., 2024). Fig. 1d shows in more detail a portion of the Fe-MOF membrane, clearly distinguishing the Fe-MOF structure wrapped and covered by the nanofibers. To confirm the attachment of Fe-MOF on the surface of the polymer fibers, an EDS mapping was performed. The results for C, O and Fe are presented in Fig. 1e, where the distribution of Fe is shown, with a higher concentration of this element found in small agglomerations evenly distributed on the membrane.

To complete the determination of the membrane composition, elemental analysis was carried out. Fig. 1e contains the table with the weight of each of the elements present in the Fe-MOF nanofiber membrane and the iron content resulted in 5%. With these results it was concluded that Fe-MOF was successfully retained in the membrane.

The wettability of the membrane was also ascertained that revealed that the membrane was completely hydrophilic, with the drop disappearing in 5 s. Fig. 1f shows an image of the drop on the fiber at 2 s into the test. As can be seen, the drop is penetrating the membrane, with the contact angle between the drop and the membrane at that time being  $62.38^\circ$  (Fig. 1g). Since this angle is less than  $90^\circ$ , it confirmed the hydrophilicity of the membrane and its high wettability. The wettability of a membrane relies on the functional groups on its surface, and the presence of amino groups in the  $\text{NH}_2$ -MIL-88(Fe) could lead to the detected enhancement (Shakiba et al., 2023).



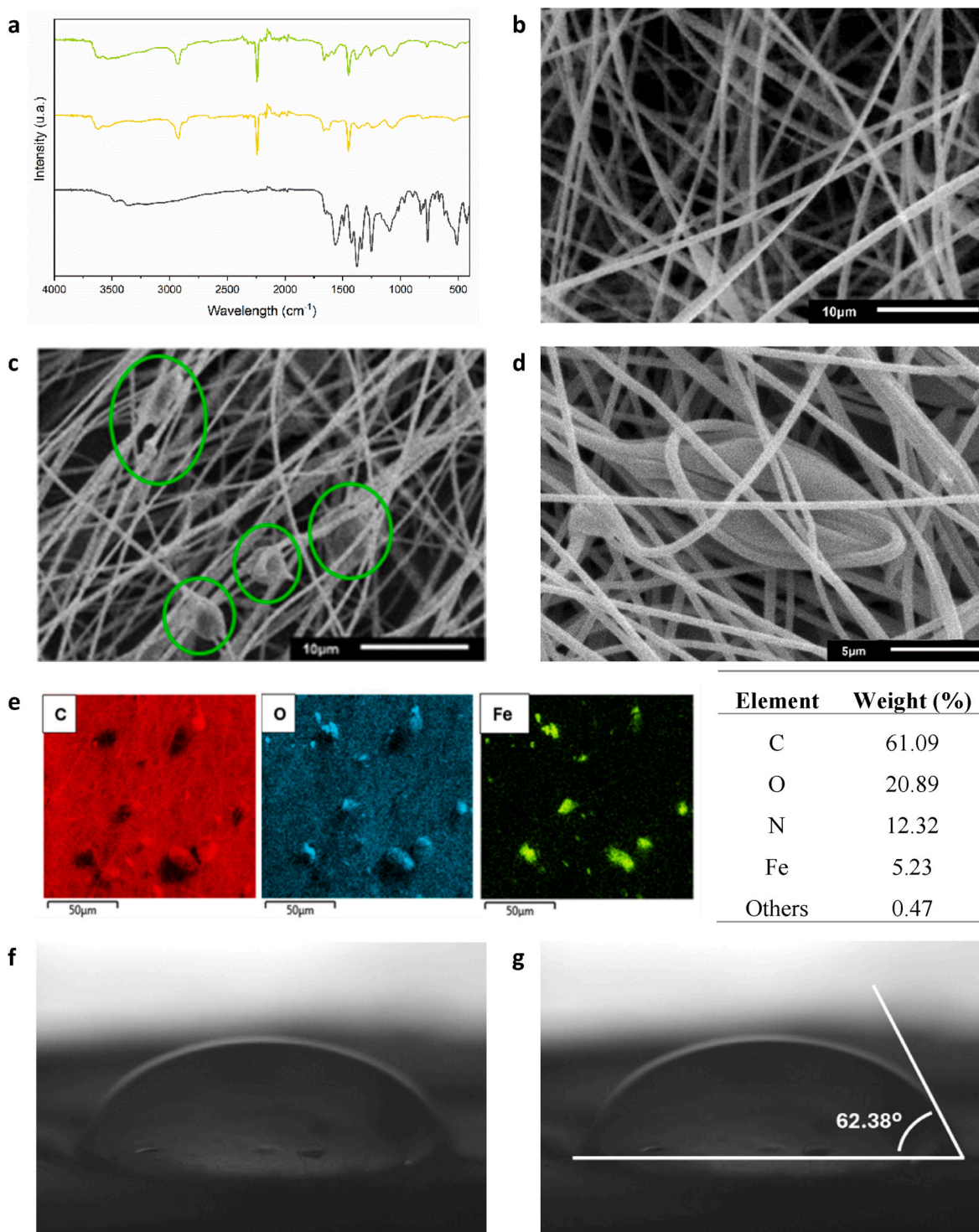


**Fig. 1.** Characterization results of obtained nanofiber membranes: a) FTIR spectra of Fe-MOF (black line), PAN membrane (orange line) and Fe-MOF nanofiber membrane (green line); b-d) SEM images of PAN membrane, and Fe-MOF nanofiber membrane with magnifications of  $\times 2,500$  and  $\times 5,000$ , respectively; e) Elemental mapping of the Fe-MOF nanofiber membrane corresponding to the elements C, O, and Fe; f) Hydrophilicity test; g) Measurement of the contact angle in the hydrophilicity test. (For interpretation of the references to colour in this figure legend, the reader is referred to the Web version of this article.)

### 3.2. Heterogeneous electro-Fenton batch process

#### 3.2.1. Heterogeneous electro-Fenton process vs anodic oxidation

Once confirmed the correct retention of the Fe-MOF on the membrane, the first step was the evaluation of SMX removal by electro-Fenton using this nanofiber membrane as a catalyst and its comparison with the simplest advanced oxidation process, anodic oxidation at

25 mA.

Prior to investigating the degradation, the SMX removal by adsorption on the Fe-MOF nanofiber membrane was ascertained resulting in a lesser part of the removal ( $< 8\%$ ) can be due to this. This slight fraction of adsorption can be related to electrostatic interactions with the SMX molecules which are mostly neutral at the solution pH  $\sim 4.5$ – $5.5$  ( $pK_{a1} = 5.86$  and  $pK_{a2} = 1.97$ ) and only a small fraction is negatively charged.



Meanwhile, PAN membrane and  $\text{NH}_2\text{-MIL-88B(Fe)}$  particles tend to be positively charged at  $\text{pH} < 6.8$  and  $8.0$ , respectively (Guo et al., 2022; Ye et al., 2022). Moreover, this adsorption can be also affected by the hydrophilic nature of the membrane and the nature of the SMX ( $\log K_{ow} = 0.89$ ).

Once the adsorption was evaluated, the SMX removal by electro-Fenton using the Fe-MOF nanofiber membrane in comparison with the anodic oxidation at  $25\text{ mA}$  was assessed (Fig. 2a). The profile of SMX concentration decreased exponentially involving a reaction with hydroxyl radicals and agreeing with of pseudo-first order kinetic model (Equation SM1).

The kinetic constants calculated for each of the treatments are presented in Fig. 2b and their values were  $0.012$  and  $0.0267\text{ min}^{-1}$ ,

respectively. It is clear the positive effect of electro-Fenton and its kinetic coefficient being twice that obtained for anodic oxidation. In addition, energy consumption (EC) decreased almost 40% when the electro-Fenton process was carried out in comparison with the anodic oxidation (Table SM2). These facts confirmed the occurrence of heterogeneous Fenton's reaction and confirmed the good catalytic activity of the elaborated Fe-MOF nanofiber membrane to decompose  $\text{H}_2\text{O}_2$  to  $\cdot\text{OH}$  radicals as reported also by He et al. (2018) in the degradation of methylene blue by Fenton catalyzed reaction.

When the results are compared with the previous ones at  $25\text{ mA}$ , the increase in applied current intensity improved SMX decay, resulting in a final degradation of 98.54% for  $100\text{ mA}$  after  $1.5\text{ h}$  of treatment in comparison with the attained 92.19% for  $25\text{ mA}$ . The generation of

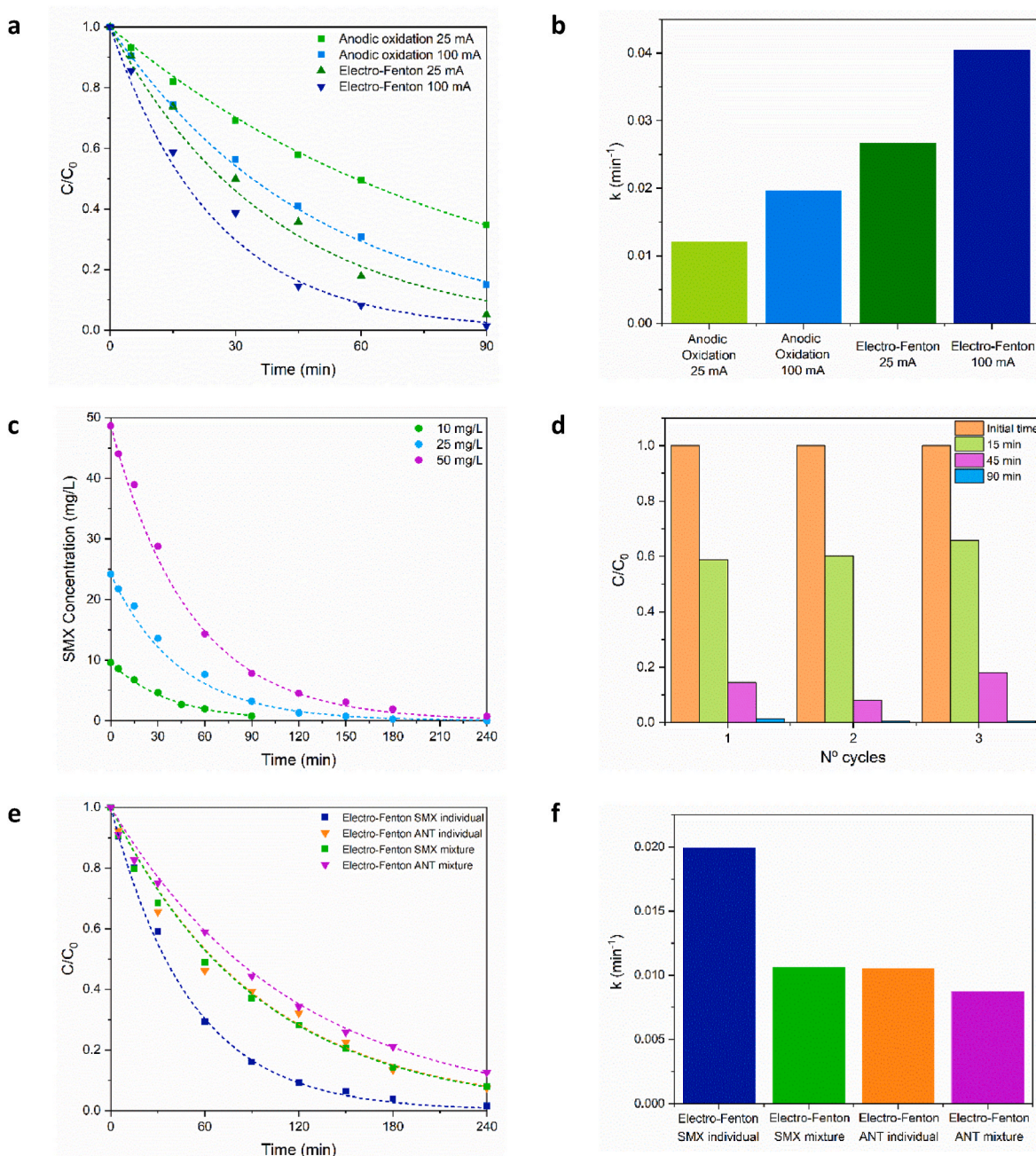


**Fig. 2.** a) Profiles of SMX degradation obtained from anodic oxidation and electro-Fenton at 25 and 100 mA; c) Profiles of SMX concentration at different initial concentration 50–10 mg/L; d) Concentration of SMX using Fe-MOF nanofiber membrane in successive cycles at different time; e) Profiles of drugs degradation obtained for electro-Fenton treatment of individual and the mixture of 50 ppm SMX and 50 ppm ANT. Dashed lines depict the pseudo-first order kinetic fitting for all experiments with a  $R^2 > 99\%$ . b) and f) Apparent pseudo-first order constant ( $k$ ) values for each experiment.

H<sub>2</sub>O<sub>2</sub> in the cathode surface can be increased when the electron transfer is increased with enough current intensity and thus the generation of hydroxyl radicals (Liu et al., 2023a). The difference in the degradation under these conditions can also be related to a greater number of generated intermediates when operating at the higher current intensity applied (Lebik-Elhadi et al., 2018; Moreira et al., 2017). Even there was an increase of 4-folds in the current intensity the attained degradation only slightly increased (less than 10%) and the kinetics were studied with an observed improvement in the reaction rate of less than 30%. Operating at a current intensity of 100 mA, the energy consumption (EC) was almost seven times higher than 25 mA to achieve only a 6% improvement in SMX elimination (Table SM2). In this case considering the elimination of SMX and EC, it was determined that a current intensity of 25 mA was the best alternative, ensuring a good efficiency of the process in removing SMX while maintaining a low energy consumption. A similar behavior related to the effect of current intensity on the degradation of pollutants was reported by del Alamo et al. (Cruz del Álamo et al., 2024) in the degradation of carbamazepine, where a 50% increase in the current intensity led to a small increase in pollutant removal by electro-Fenton.

### 3.2.2. Effect of the SMX concentration

The behavior of the system was studied by testing initial concentrations of SMX of 10–50 mg/L without varying the amount of catalyst and obtaining their degradation profiles (Fig. 2c). The results indicated that, as the initial SMX concentration increased its degradation efficiency showed a decreasing trend at the same reaction times. In particular, the initial SMX concentrations of 10, 25 and 50 mg/L decreased to 1.96, 7.64 and 14.30 mg/L respectively after 1 h of treatment. The SMX degradation followed a pseudo-first order kinetic with the rate constants showing the same trend. Increasing the concentration of SMX requires the presence of more hydroxyl radicals in the solution for the degradation reaction to take place. At the same time, increased initial SMX concentration led to increased intermediates formed during the degradation process, which would compete with SMX by radicals (Song et al., 2024; Zou et al., 2022). These two reasons mainly influence the slowness of the process when the initial pollutant concentration is increased. Even so, the system showed a significant and high oxidation potential for a high concentration of contaminant, which allowed an efficient elimination of the drug in a short treatment duration.

The EC was also affected by the increase in the initial concentration of SMX (Table SM2). After 90 min of treatment at 25 mA, the EC values obtained for 10, 25 and 50 mg/L of SMX were 0.299, 0.113 and 0.064 kWh/g respectively. The results indicated that as the initial pollutant concentration increased, consumption decreased, but the degradation obtained was also lower.

### 3.2.3. Stability and reusability of the Fe-MOF nanofiber membranes

To evaluate the reusability of this material, three electro-Fenton cycles were carried out at the highest evaluated current intensity (100 mA) to ensure the behavior and resistance of the fiber in order to simulate the more extreme conditions than would be used to perform the continuous system (Fig. 2d).

As seen in Fig. 2d, the catalytic capacity of Fe-MOF fiber membrane maintains practically constant during the three cycles carried out, achieving almost total degradation of the contaminant, which makes it suitable for multiple reuses. The slight loss in the performance of the Fe-MOF nanofiber membrane could be related to the deactivation and exfoliation of some of Fe-MOF particles retained into the membrane (Ye et al., 2022). In addition, an analysis of the iron content in the liquid phase was carried out for each cycle to determine possible leaching of the material, and it was found a minimal release of this metal, less than 0.5%, which explains the small variation in drug elimination efficiency. Moreover, during this study, it was observed that the Fe-MOF nanofiber membrane remains intact after being used several times; it didn't undergo breakage or deformations. Therefore, the viability of this material

to be used in a continuous electro-Fenton system was confirmed.

### 3.2.4. Effect of the mixture of drugs (SMX and ANT) on the removal

Normally, wastewater contains more than one pollutant. So, before implementing the continuously system, a test was made with a mixture of two drugs, SMX and ANT. Thus, the degradation profiles resulting from electro-Fenton treatment are presented for each drug separately and for the mixture of both (Fig. 2e). The corresponding kinetic constants, calculated by a pseudo-first order kinetic adjustment, are shown in Fig. 2f.

Analyzing the values obtained for the SMX, it was clearly seen that the degradation is much faster when treated individually than in the mixture (Fig. 2e), being the value of the kinetic constant obtained practically double, 0.0199 min<sup>-1</sup> for individual treatment versus 0.0106 min<sup>-1</sup> for mixing. Also, individual treatment obtained a degradation of 96.07% after 3 h of treatment, while in the case of the mixture 92.10% degradation of SMX was achieved at the end of the treatment (Table SM3). However, in the case of ANT the difference was not so remarkable, the degradation profiles were quite similar in both cases throughout the treatment, reaching a final degradation of 92.54% and 87.43% when treated individually and in the mixture respectively. Therefore, efficiency in the case of ANT decreased by 5.1% when treated in the mixture.

On the other hand, when the results obtained for both drugs present in the mixture were compared, it could be seen that the degradation profile obtained throughout the treatment was very similar for both, reaching a final degradation of 92.10% SMX and 87.43% ANT. The apparent kinetic constants for both molecules were very close, being 0.0106 min<sup>-1</sup> and 0.0087 min<sup>-1</sup> for SMX and ANT, respectively. This shows that hydroxyl radicals really acted as non-selective oxidants in this case.

Finally, analyzing the calculated consumption for these trials (Table SM3) it was observed that the total consumption in the case of the mixture (0.318 kWh/g) was greater than in the individual treatment of the drugs. This is justifiable given that the total load of pollutants to be treated was double. In addition, if the consumption values obtained for the individual electro-Fenton of SMX and ANT are added, a result of 0.317 kWh/g is obtained, practically the same as in the case of the mixture, since the degradation achieved is very similar in both cases for both drugs.

### 3.2.5. Degradation pathway of SMX and ANT

The degradation process involves the participation of several ROS that can be generated in the electro-Fenton process. Thus, scavenging assays were conducted to evaluate the major oxidizing species during drug oxidation. Different quenchers agents were used, TBA for hydroxyl radicals, FFA for both hydroxyl radicals and singlet, and PBQ for superoxide radicals (Larralde-Piña et al., 2023; Zhang et al., 2022). It is possible to evaluate their relative contribution to the drug degradation mechanism. In the case study, TBA showed an inhibitory effect of 78.6%, which confirms that hydroxyl radicals are the main contributors to drug degradation and underscores the efficiency of the electro-Fenton process in generating these radicals from H<sub>2</sub>O<sub>2</sub>. In the case of superoxide its contribution was lower inhibiting 13.1% and, finally, singlet was the one that showed a lower effect, with 8.3% (Figure SM4).

The transformation of the pollutants mixture into the mineralized products was monitored by the TOC reduction profile. As shown in Fig. 3a, the TOC decreased along the time, and this decrease was related to the appearance phenols (Fig. 3b) and carboxylic acids which were the last step before mineralization. It can be observed that the carboxylic acids appeared at the beginning (15 min), increased until 90 min and after that decreased following a mineralization process. The reached TOC removal after 240 min was higher than 70% with the of carboxylic acids being almost 90% of the organic content of the sample. This fact indicated that the pollutants were almost completely degraded, and the generated intermediates mostly mineralized.



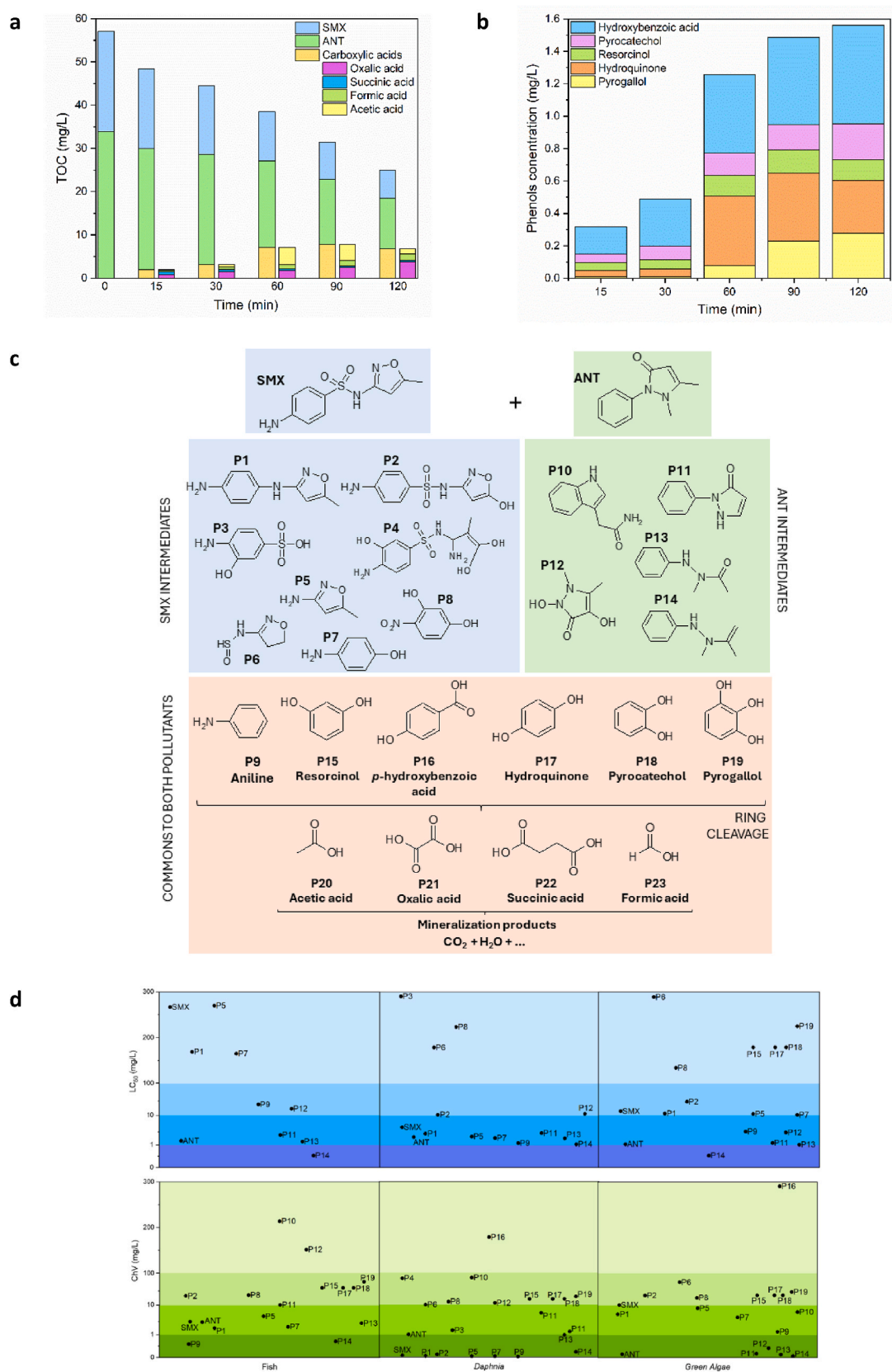


**Fig. 3.** a) TOC profiles including carboxylic acids obtained for electro-Fenton treatment of the mixture of 50 ppm SMX and 50 ppm ANT; b) Intermediate phenol profiles obtained for electro-Fenton treatment of the mixture of 50 ppm SMX and 50 ppm ANT; c) Proposed degradation pathway for electro-Fenton treatment of the mixture of 50 ppm SMX and 50 ppm ANT; d)  $LC_{50}$  toxicity and ChV toxicity obtained via ECOSAR 2.2. Values < 1 mg/L would mean very toxic, 1–10 mg/L toxic, 10–100 mg/L harmful and >100 not harmful.



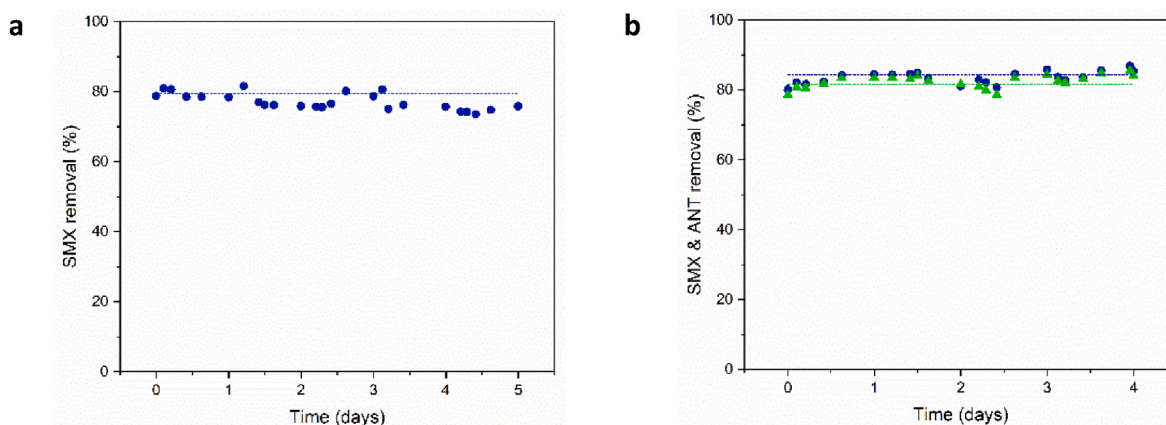


**Fig. 4.** Profiles of pollutant degradation obtained from the continuous electro-Fenton process once the system reached stability for an initial inlet solution of: a) 50 ppm SMX; b) A mixture consisting of 50 ppm SMX and 50 ppm ANT.

Based on the different degradation intermediates identified during the degradation process, a plausible degradation pathway was proposed (Fig. 3c). Different intermediates related to SMX (compounds P1–P8) and ANT (compounds P10–P14) degradation, as well as common intermediates to both (compounds P9 and P15–P23), appeared during the degradation process. These compounds suggested that different degradation pathways were followed in the presence of the hydroxyl radicals.

In a final step, these intermediates undergo the rupture and opening of the aromatic ring, which leads to the production of short-chain carboxylic acids and inorganic ions (Liu et al., 2023a; Tesnim et al., 2024). Several carboxylic acids were identified such as oxalic, succinic, formic and acetic acid (P20–P23). Analyzing the results obtained for carboxylic acids, their concentration showed a slight tendency to increase and then decrease (Figure SM5). Specifically, these acids will degrade into CO<sub>2</sub> and H<sub>2</sub>O. Therefore, the detection of these products, phenols and carboxylic, confirmed the progressive degradation of the drugs.

### 3.2.6. Toxicity evaluation

The toxicity of the pollutants and their degradation products needs to be evaluated. In some cases, the generated intermediates are more harmful than the parent compounds (Song et al., 2024). Therefore, the environmental impact assessment of the pollutants and their identified intermediates was predicted by ECOSAR program (Fig. 3d and Table SM4). It should be considered that the lower the values of LC<sub>50</sub> toxicity and ChV toxicity, the higher the toxicity of the intermediates (Song et al., 2024; Wang et al., 2022). Thus, values < 1 mg/L would mean very toxic, 1–10 mg/L toxic, 10–100 mg/L harmful and >100 not harmful.

Analyzing the results obtained for LC<sub>50</sub> toxicity, was observed that ANT was more harmful than SMX for the three cases, fish, *Daphnia* and *Green Algae*. Accordingly, ANT intermediates showed higher toxicity, with P14 being the most notable. In the case of ChV toxicity, both SMX and ANT showed a higher toxicity, as well as their intermediates products, being mostly very toxic, toxic or harmful for the three individuals studied. The degradation of these intermediates products resulted in the formation of phenols and carboxylic acids. The results of the predicted ecotoxicity showed that the detected phenols and the carboxylic acids (P15–23) were not harmful. Thus, the toxicity to the environment would disappear with the mineralization.

### 3.3. Continuous electro-Fenton process

Nowadays, most industrial processes operate continuously, generating constant flows of pollutants, as would be the case with wastewater from the pharmaceutical industry. Therefore, it is necessary to test the materials obtained at laboratory level in long-lasting systems and

processes to assess the feasibility of their application on a larger scale (Rosales et al., 2009).

The system configuration as well as the parameters used were explained in section 2.4.2. In this case, the Fe-MOF nanofiber membrane had to fulfill two functions. First, act as a filter since the contaminating solution must pass through it, retaining the larger particles and, secondly, act as catalyst of the electro-Fenton process.

Two tests were performed operating continuously. The system was first tested using an inlet solution with a concentration of 50 ppm SMX and a residence time of 3.35 h. Then, it was tested with a mixture of 50 ppm SMX and 50 ppm ANT with a residence time of 8.5 h. Fig. 4a and b show the degradation profiles over the treatment time after the system reached stabilization for each of the tests, respectively.

Analyzing the results obtained, in both tests it can be seen how, once the system reached stabilization, the degradation remained constant throughout the experiment, indicating that the membrane maintained its catalytic activity during this time. In the case of SMX solution (Fig. 4a), degradation remained between 78 and 82% during the 5 days. For the mixture of SMX and ANT (Fig. 4b), the pollutant load was higher, so the residence time was increased to achieve a degradation similar to that of the first test. The degradation obtained for each of the drugs varied between 80 and 85% during the 4 days. In both cases, the membrane was recovered at the end of the experiment, it was observed that the material didn't present damage or deformations, remaining intact throughout the treatment. This confirms that the membrane is resistant and maintains its catalytic activity in long-term treatments.

Finally, the formation of carboxylic acids resulting from the oxidative degradation of drugs in the processes carried out continuously were analyzed (Figure SM6). In both cases, the same trend was observed, the quantity of each of the acids remained constant during the process, since it is a continuous process, this trend is consistent. In addition, should be noted that in the case of 50 ppm SMX continuous treatment, the TOC went from 20.7 mg/L to 5.6 mg/L after the experiment, of this amount 1.59 mg/L correspond to carboxylic acids. In the case of the treatment of the mixture formed by 50 ppm of SMX and 50 ppm of ANT the TOC decreases from 55.7 mg/L to 8.75 mg/L, representing the carboxylic acids 2.15 mg/L of that amount. Therefore, can be concluded that in both cases the reduction of TOC is highly significant, which implies a good degradation of the drugs and therefore a good continuous functioning of the electro-Fenton system incorporating the synthesized Fe-MOF nanofiber membrane as catalyzed.

## 4. Conclusions

In this work, the synthesis and successful integration of a Fe-MOF into a nanofiber membrane were achieved via the electrospinning

technique. Characterization confirmed Fe-MOF presence and stability within the membrane nanofibers. Moreover, this nanofiber membrane demonstrated significant catalytic activity in the heterogeneous electro-Fenton process, effectively degrading contaminants such as SMX and ANT in batch assays. The study revealed that several operational parameters, including current intensity and initial drug concentration, significantly impact the efficiency of the electro-Fenton degradation process. Optimal operational conditions ensured high efficiency in the elimination of SMX and ANT while maintaining low energy consumption.

The influence of ROS on the degradation mechanism was also investigated, highlighting hydroxyl radicals as the primary contributors to mineralization process and underscores the efficiency of the electro-Fenton process in the toxicity reduction availed by in-silico assays.

Additionally, the membrane proved high reusability and stability that was confirmed by its feasible application in continuous electro-Fenton systems and attaining significant degradation over extended periods. This work provides a foundation for future research into optimizing and scaling this technology for broader environmental applications.

### CRedit authorship contribution statement

**Barbara Lomba-Fernández:** Writing – original draft, Visualization, Investigation, Conceptualization. **Antía Fdez-Sanromán:** Writing – review & editing, Visualization, Investigation, Conceptualization. **Marta Pazos:** Writing – review & editing, Validation, Resources, Formal analysis. **M. Angeles Sanromán:** Writing – review & editing, Validation, Supervision, Resources, Project administration, Methodology, Funding acquisition, Conceptualization. **Emilio Rosales:** Writing – review & editing, Validation, Software, Formal analysis, Data curation.

### Declaration of competing interest

The authors declare that they have no known competing financial interests or personal relationships that could have appeared to influence the work reported in this paper.

### Data availability

Data will be made available on request.

### Acknowledgments

The acknowledgments to be included in this section are the following: This research has been supported by R&D Project PCI2022-132941 and TED2021-129590A-I00 funded by MICIU/AEI/10.13039/501100011033 and by the European Union Next Generation EU/PRTR. Xunta de Galicia and European Regional Development Fund for their support in project ED431C 2021-43. R&D Project PID2020-113667 GB-I00 funded by MICIU/AEI/10.13039/501100011033. Also, Antía Fdez-Sanromán thanks MICIU/AEI/10.13039/501100011033 and FSE+ (PRE2021-098540). Funding for open access charge: Universidade de Vigo/CISUG.

### Appendix A. Supplementary data

Supplementary data to this article can be found online at <https://doi.org/10.1016/j.chemosphere.2024.143447>.

### References

- Agarwal, S., Wendorff, J.H., Greiner, A., 2008. Use of electrospinning technique for biomedical applications. *Polymer* (Guildf). <https://doi.org/10.1016/j.polymer.2008.09.014>.
- Badea, S.L., Niculescu, V.C., 2022. Recent progress in the removal of legacy and emerging organic contaminants from wastewater using metal-organic frameworks: an overview on adsorption and catalysis processes. *Materials*. <https://doi.org/10.3390/ma15113850>.
- Bhardwaj, N., Kundu, S.C., 2010. Electrospinning: a fascinating fiber fabrication technique. *Biotechnol. Adv.* <https://doi.org/10.1016/j.biotechadv.2010.01.004>.
- Boorboor Ajdari, F., Kowsari, E., Niknam Shahrak, M., Ehsani, A., Kiaei, Z., Torkzaban, H., Ershadi, M., Kholghi Eshkalak, S., Haddadi-Asl, V., Chinnappan, A., Ramakrishna, S., 2020. A review on the field patents and recent developments over the application of metal organic frameworks (MOFs) in supercapacitors. *Coord. Chem. Rev.* <https://doi.org/10.1016/j.ccr.2020.213441>.
- Brillas, E., 2022. Fenton, photo-Fenton, electro-Fenton, and their combined treatments for the removal of insecticides from waters and soils. A review. *Sep Purif Technol.* <https://doi.org/10.1016/j.seppur.2021.120290>.
- Cruz del Álamo, A., Puga, A., Dias Soares, C.M., Pariente, M.I., Pazos, M., Molina, R., Sanromán, M.A., Martínez, F., Delerue-Matos, C., 2024. Novel 3D electro-Fenton reactor based on a catalytic packed bed reactor of perovskite/carbon microelectrodes for the removal of carbamazepine in wastewater. *J. Environ. Chem. Eng.* 12. <https://doi.org/10.1016/j.jece.2024.113154>.
- dos Santos, A.J., Kronka, M.S., Fortunato, G.V., Lanza, M.R.V., 2021. Recent advances in electrochemical water technologies for the treatment of antibiotics: a short review. *Curr. Opin. Electrochem.* <https://doi.org/10.1016/j.coelec.2020.100674>.
- Du, X., Fu, W., Su, P., Zhang, Q., Zhou, M., 2023. FeMo@porous carbon derived from MIL-53(Fe)/MoO<sub>3</sub> as excellent heterogeneous electro-Fenton catalyst: Co-catalysis of Mo. *J. Environ. Sci. (China)* 127, 652–666. <https://doi.org/10.1016/j.jes.2022.06.031>.
- Du, X., Wang, S., Ye, F., Qingrui, Z., 2022. Derivatives of metal-organic frameworks for heterogeneous Fenton-like processes: from preparation to performance and mechanisms in wastewater purification – a mini review. *Environ. Res.* 206. <https://doi.org/10.1016/j.envres.2021.112414>.
- Du, X., Zhou, M., 2021. Strategies to enhance catalytic performance of metal-organic frameworks in sulfate radical-based advanced oxidation processes for organic pollutants removal. *Chem Eng J.* <https://doi.org/10.1016/j.cej.2020.126346>.
- Fdez-Sanromán, A., Lomba-Fernández, B., Sanromán, A., Pazos, M., Rosales, E., 2024. Enhancing stability and immobilization techniques for graphitic carbon nitride in photocatalytic applications. *J. Mol. Liq.* 405, 125005. <https://doi.org/10.1016/j.molliq.2024.125005>.
- Fdez-Sanromán, A., Pazos, M., Sanromán, M.A., Rosales, E., 2023a. Heterogeneous electro-Fenton system using Fe-MOF as catalyst and electrocatalyst for degradation of pharmaceuticals. *Chemosphere* 340. <https://doi.org/10.1016/j.chemosphere.2023.139942>.
- Fdez-Sanromán, A., Rosales, E., Pazos, M., Sanromán, A., 2023b. One-pot synthesis of bimetallic Fe-Cu metal-organic frameworks composite for the elimination of organic pollutants via peroxymonosulphate activation. *Environ Sci Pollut R.* <https://doi.org/10.1007/s11356-023-30026-5>.
- Fdez-Sanromán, A., Rosales, E., Pazos, M., Sanromán, A., 2022. Metal-organic frameworks as powerful heterogeneous catalysts in advanced oxidation processes for wastewater treatment. *Appl. Sci.* <https://doi.org/10.3390/app12168240>.
- Fu, A., Liu, Z., Sun, Z., 2022. Cu/Fe oxide integrated on graphite felt for degradation of sulfamethoxazole in the heterogeneous electro-Fenton process under near-neutral conditions. *Chemosphere* 297. <https://doi.org/10.1016/j.chemosphere.2022.134257>.
- Gong, X.Y., Huang, Z.H., Zhang, H., Liu, W.L., Ma, X.H., Xu, Z.L., Tang, C.Y., 2020. Novel high-flux positively charged composite membrane incorporating titanium-based MOFs for heavy metal removal. *Chem Eng J* 398. <https://doi.org/10.1016/j.cej.2020.125706>.
- Gopinath, A., Pisharody, L., Popat, A., Nidheesh, P.V., 2022. Supported catalysts for heterogeneous electro-Fenton processes: recent trends and future directions. *Curr. Opin. Solid State Mater. Sci.* <https://doi.org/10.1016/j.cossms.2022.100981>.
- Guo, W., Guo, R., Pei, H., Wang, B., Liu, N., Mo, Z., 2022. PAN/PEI nanofiber membrane for effective removal of heavy metal ions and oil-water separation. *J. Polym. Environ.* 30, 4835–4847. <https://doi.org/10.1007/s10924-022-02541-y>.
- He, J., Zhang, Y., Zhang, X., Huang, Y., 2018. Highly efficient Fenton and enzyme-mimetic activities of NH<sub>2</sub>-MIL-88B(Fe) metal organic framework for methylene blue degradation. *Sci. Rep.* 8. <https://doi.org/10.1038/s41598-018-23557-2>.
- Heidari, Z., Pelalak, R., Zhou, M., 2023. A critical review on the recent progress in application of electro-Fenton process for decontamination of wastewater at near-neutral pH. *Chem Eng J.* <https://doi.org/10.1016/j.cej.2023.145741>.
- Huang, Y.H., Liu, Y., Du, P.P., Zeng, L.J., Mo, C.H., Li, Y.W., Lü, H., Cai, Q.Y., 2019. Occurrence and distribution of antibiotics and antibiotic resistant genes in water and sediments of urban rivers with black-odor water in Guangzhou, South China. *Sci. Total Environ.* 670, 170–180. <https://doi.org/10.1016/j.scitotenv.2019.03.168>.
- Hussain, M., Salam, A., Arain, M.F., Ullah, A., Dao, A.T., Vu-Manh, H., Phan, D.N., Ansari, A.S., Khan, M.Q., Javed, Z., Kim, I.S., 2021. Polyacrylonitrile nanofibers containing virobloc as promising material for protective clothing. *Appl. Sci.* 11. <https://doi.org/10.3390/app112311469>.
- Jin, E., Lee, S., Kang, E., Kim, Y., Choe, W., 2020. Metal-organic frameworks as advanced adsorbents for pharmaceutical and personal care products. *Coord. Chem. Rev.* <https://doi.org/10.1016/j.ccr.2020.213526>.
- Khalif, A., Madhally, S.V., 2017. Recent advances in multi-axial electrospinning for drug delivery. *Eur. J. Pharm. Biopharm.* <https://doi.org/10.1016/j.ejpb.2016.11.010>.
- Laralde-Piña, I.A., Acuña-Askar, K., Villanueva-Rodríguez, M., Guzmán-Mar, J.L., Murillo-Sierra, J.C., Ruiz-Ruiz, E.J., 2023. An optimized electro-fenton pretreatment for the degradation and mineralization of a mixture of ofloxacin, norfloxacin, and ciprofloxacin. *Chemosphere* 344. <https://doi.org/10.1016/j.chemosphere.2023.140339>.
- Lebik-Elhadi, H., Frontistis, Z., Ait-Amar, H., Amrani, S., Mantzavinos, D., 2018. Electrochemical oxidation of pesticide thiamethoxam on boron doped diamond

- anode: role of operating parameters and matrix effect. *Process Saf Environ Prot* 116, 535–541. <https://doi.org/10.1016/j.psep.2018.03.021>.
- Li, Y., Zhu, J., Cheng, H., Li, G., Cho, H., Jiang, M., Gao, Q., Zhang, X., 2021. Developments of advanced electrospinning techniques: a critical review. *Adv Mater Technol.* <https://doi.org/10.1002/admt.202100410>.
- Liu, D., Chen, D., Jiang, L., Hao, Z., Tan, R., Deng, B., Wang, Y., Tian, Y., Chen, L., Jia, B., 2023a. Efficient degradation of sulfamethoxazole in heterogeneous Electro-Fenton process with CeO<sub>2</sub>@MoS<sub>2</sub>@GF modified cathode: mechanism and degradation pathway. *Sep. Purif. Technol.* 320. <https://doi.org/10.1016/j.seppur.2023.124212>.
- Liu, G., Luo, D., Wang, L., Wang, C., Cao, Y., Singh, L., Ahmadzadeh, S., He, Z., 2023b. Current status and future perspective in electro-Fenton techniques for wastewater treatment: a bibliometric review. *Appl. Nanosci.* <https://doi.org/10.1007/s13204-023-02855-w>.
- Liu, M., Zhang, L., Wang, M., Wang, X., Cui, H., Wei, J., Li, X., 2023c. The role of metal-organic frameworks in removing emerging contaminants in wastewater. *J. Clean. Prod.* <https://doi.org/10.1016/j.jclepro.2023.139526>.
- Moreira, F.C., Boaventura, R.A.R., Brillas, E., Vilar, V.J.P., 2017. Electrochemical advanced oxidation processes: a review on their application to synthetic and real wastewaters. *Appl. Catal., B.* <https://doi.org/10.1016/j.apcatb.2016.08.037>.
- Oladoye, P.O., Adegboyega, S.A., Giwa, A.R.A., 2021. Remediation potentials of composite metal-organic frameworks (MOFs) for dyes as water contaminants: a comprehensive review of recent literatures. *Environ. Nanotechnol. Monit. Manag.* <https://doi.org/10.1016/j.enmm.2021.100568>.
- Petit, C., 2018. Present and future of MOF research in the field of adsorption and molecular separation. *Curr Opin Chem Eng.* <https://doi.org/10.1016/j.coche.2018.04.004>.
- Pujiarti, H., Pangestu, Z.A., Sholeha, N., Nasikhudin, N., Diantoro, M., Utomo, J., Aziz, M.S.A., 2023. The effect of acetylene carbon black (ACB) loaded on polyacrylonitrile (PAN) nanofiber membrane electrolyte for DSSC applications. *Micromachines* 14. <https://doi.org/10.3390/mi14020394>.
- Ramezani, M.R., Ansari-Asl, Z., Hoveizi, E., Kiasat, A.R., 2020. Fabrication and characterization of Fe(III) metal-organic frameworks incorporating polycaprolactone nanofibers: potential scaffolds for tissue engineering. *Fibers Polym.* 21, 1013–1022. <https://doi.org/10.1007/s12221-020-9523-6>.
- Rojas, S., Horcajada, P., 2020. Metal-organic frameworks for the removal of emerging organic contaminants in water. *Chem Rev.* <https://doi.org/10.1021/acs.chemrev.9b00797>.
- Rosales, E., Pazos, M., Longo, M.A., Sanromán, M.A., 2009. Electro-Fenton decoloration of dyes in a continuous reactor: a promising technology in colored wastewater treatment. *Chem Eng J* 155, 62–67. <https://doi.org/10.1016/j.cej.2009.06.028>.
- Shakiba, M., Abdouss, M., Mazinani, S., Reza Kalaei, M., 2023. Super-hydrophilic electrospun PAN nanofibrous membrane modified with alkaline treatment and ultrasonic-assisted PANI in-situ polymerization for highly efficient gravity-driven oil/water separation. *Sep. Purif. Technol.* 309. <https://doi.org/10.1016/j.seppur.2022.123032>.
- Sharabati, M. Al, Sabouni, R., Hussein, G.A., 2022. Biomedical applications of Metal–Organic frameworks for disease diagnosis and drug delivery: a review. *Nanomaterials.* <https://doi.org/10.3390/nano12020277>.
- Sirés, I., Brillas, E., 2021. Upgrading and expanding the electro-Fenton and related processes. *Curr. Opin. Electrochem.* <https://doi.org/10.1016/j.coelec.2020.100686>.
- Song, G., Su, P., Zhang, Q., Zhou, M., 2022. Interface regulation in electro-Fenton for efficient environmental remediation. *Curr. Opin. Electrochem.* <https://doi.org/10.1016/j.coelec.2022.101163>.
- Song, Y., Wang, A., Ren, S., Zhang, Y., Fan, R., Liu, Y., Zhang, Z., 2024. Electro-controlled membrane coupling heterogeneous electro-Fenton (EM-HEF) in treating acetaminophen: performance, mechanism, DFT calculation, and application. *Sep. Purif. Technol.* 345. <https://doi.org/10.1016/j.seppur.2024.127345>.
- Subash, A., Naebe, M., Wang, X., Kandasubramanian, B., 2022. Fabrication of biodegradable fibrous systems employing electrospinning technology for effluent treatment. *Environmental Science: Advances.* <https://doi.org/10.1039/d2va00244b>.
- Szekeres, E., Chiriac, C.M., Baricz, A., Szőke-Nagy, T., Lung, I., Soran, M.L., Rudi, K., Dragos, N., Coman, C., 2018. Investigating antibiotics, antibiotic resistance genes, and microbial contaminants in groundwater in relation to the proximity of urban areas. *Environ Pollut* 236, 734–744. <https://doi.org/10.1016/j.envpol.2018.01.107>.
- Tang, M., Wan, J., Wang, Y., Ye, G., Yan, Z., Ma, Y., Sun, J., 2024. Overlooked role of void-nanoconfined effect in emerging pollutant degradation: modulating the electronic structure of active sites to accelerate catalytic oxidation. *Water Res.* 249. <https://doi.org/10.1016/j.watres.2023.120950>.
- Tesnim, D., Díez, A.M., Amor Hédi, B., Sanroman, M.A., Pazos, M., 2024. Sustainable removal of antipyrine from wastewater via an Eco-Friendly heterogeneous Electro-Fenton-like process employing Zero-Valent iron nanoparticles loaded activated carbon. *Chem Eng J* 493. <https://doi.org/10.1016/j.cej.2024.152494>.
- Uddin, Z., Ahmad, F., Ullan, T., Nawab, Y., Ahmad, S., Azam, F., Rasheed, A., Zafar, M.S., 2022. Recent trends in water purification using electrospun nanofibrous membranes. *Int. J. Environ. Sci. Technol.* <https://doi.org/10.1007/s13762-021-03603-9>.
- Wang, J., Qin, J., Liu, B., Song, S., 2022. Reaction mechanisms and toxicity evolution of Sulfamethoxazole degradation by CoFe-N doped C as Electro-Fenton cathode. *Sep. Purif. Technol.* 298. <https://doi.org/10.1016/j.seppur.2022.121655>.
- Ye, Z., Oriol, R., Yang, C., Sirés, I., Li, X.Y., 2022. A novel NH<sub>2</sub>-MIL-88B(Fe)-modified ceramic membrane for the integration of electro-Fenton and filtration processes: a case study on naproxen degradation. *Chem Eng J* 433. <https://doi.org/10.1016/j.cej.2021.133547>.
- Yu, S., Pang, H., Huang, S., Tang, H., Wang, S., Qiu, M., Chen, Z., Yang, H., Song, G., Fu, D., Hu, B., Wang, X., 2021. Recent advances in metal-organic framework membranes for water treatment: a review. *Sci. Total Environ.* <https://doi.org/10.1016/j.scitotenv.2021.149662>.
- Zhang, F., Li, Y., Ding, B., Shao, G., Li, N., Zhang, P., 2023. Electrospinning photocatalysis meet in situ irradiated XPS: recent mechanisms advances and challenges. *Small.* <https://doi.org/10.1002/smll.202303867>.
- Zhang, H., Quan, L., Gao, A., Tong, Y., Shi, F., Xu, L., 2020. Thermal analysis and crystal structure of poly(acrylonitrile-co-itaconic acid) copolymers synthesized in water. *Polymers* 12. <https://doi.org/10.3390/polym12010221>.
- Zhang, L., Wen, X., Ming, Q., Luo, X., He, T., Chen, T., Jiang, M., Wang, M., Ma, L., 2024. One-step prepared multifunctional polyacrylonitrile/MIL-100(Fe) membrane with high-density porous fibers for efficient dye/oil wastewater remediation. *Langmuir* 40, 6550–6561. <https://doi.org/10.1021/acs.langmuir.4c00230>.
- Zhang, T., Sun, L., Sun, X., Dong, H., Yu, Han, Yu, Hongbing, 2022. Radical and non-radical cooperative degradation in metal-free electro-Fenton based on nitrogen self-doped biochar. *J. Hazard Mater.* 435. <https://doi.org/10.1016/j.jhazmat.2022.129063>.
- Zou, Y., Qi, H., Sun, Z., 2022. In-situ catalytic degradation of sulfamethoxazole with efficient CuCo–O@CNTs/NF cathode in a neutral electro-Fenton-like system. *Chemosphere* 296. <https://doi.org/10.1016/j.chemosphere.2022.134072>.